

CLNS-273
June 1974Test of Scale Invariance in High Energy Muon Interactions^{*}D. J. Fox⁺, C. Chang, K. W. Chen, A. Kotlewski, P. F. Kunz⁺Michigan State University,
East Lansing, Michigan 48823

L. N. Hand, S. Herb, S. C. Loken, A. Russell, Y. Watanabe

Cornell University, Ithaca, New York 14850

W. Vernon

University of California at San Diego,
La Jolla, California 92037M. Strovink^{**}

Princeton University, Princeton, New Jersey 08540

^{*} Supported by National Science Foundation Grants GP 59070,
GP 32565, and GP 28317.⁺ Deceased.[‡] Now at Stanford Linear Accelerator Center, Stanford,
California 94305.^{**} Visiting Assistant Professor, Cornell University, 1971-72.
Now at the University of California, Berkeley, California
94720.

Some years ago, Bjorken predicted¹ that the structure functions in the deep inelastic scattering of leptons from nucleons, although nominally a function of two variables q^2 and ω ,² would, in the limit $q^2/v^2 \rightarrow 0$, be a function of ω only. This concept³ of scale invariance and the subsequent experimental evidence for its validity discovered at SLAC³ led to many predictions based on a hypothetical point-like character of the constituents of the proton and neutron, usually called the parton model.⁴ Recent studies have indicated theoretical reasons may exist, specifically in gauge theories,⁵ for modifications to the original prediction that no q^2 dependence would be observed in $F_2(q^2, \omega)$. These modifications permit a weak q^2 dependence.

It is of interest to test the concept of scale invariance at the higher energies now available at the Fermi National Accelerator Laboratory in order to see whether the apparent point-like nature of the constituents is maintained with the shorter distances resolved at these higher energies.

For technical reasons it was easier to perform the experiment with muons rather than electrons. The simplest and most direct form of scaling test would be to measure $d^2\sigma/d\Omega dE$ ⁶ at different incident muon energies for the same q^2 and ω values. This would allow separation of the structure

functions, usually parameterized as ($F_2 = vW_2$, $R = \sigma_s/\sigma_t$). F_2 could then be plotted vs. q^2 at fixed ω for different ω values. Such a method requires very high beam intensities and long running times to achieve sufficient statistical accuracy. In this muon scattering experiment we are faced with muon beam intensities 7-8 orders of magnitude less than the (lower energy) electron fluxes available at SLAC. About 2-3 orders of magnitude can be compensated by the use of thicker targets to scatter muons, but there is still a need to find a method which makes efficient use of the available small number of muons.

In the experiment reported here⁷, 56.3 and 150 GeV muons are scattered from an iron target and momentum analyzed using a spectrometer consisting of magnetized iron toroids. The scaling test is made by comparing measured distributions in q^2 at these two incident muon energies, or by separate comparison with Monte Carlo predictions based on the SLAC results. Although it is necessary in principle to assume the form of R in order to interpret the results, in practice it makes little difference. A method was devised which compensates for variation of the kinematic range accepted by the spectrometer through simultaneous variation of the apparatus geometry with the beam energy. Requiring both the acceptance region and

spectrometer multiple scattering to be nearly identical at all measured points along the scattered muon trajectory essentially determines both the geometric configuration and the ratio of the two incident energies.⁸ It is possible to satisfy all of these conditions everywhere only because $\frac{\sqrt{3}}{3} = \frac{\sqrt{8}}{5}$ to about 2%. The relative energies are then in the ratio 3:8 as is the amount of scattering material, while the actual bending power, i.e. magnetized part of the spectrometer, changes in the ratio 3:5. The target obeys a similar scaling relation and the final result is an apparatus which is almost bias free in the test of scaling made by direct comparison of q^2 distributions at 56.3 and 150 GeV. To a large extent this design for the apparatus makes it possible to minimize variations in the acceptance and "edge" effects due to scattering in or out of the finite spectrometer aperture.

It should be emphasized that the scaling test reported here uses an iron target. Previous work with electrons⁹ and muons¹⁰ showed that no deviations from simple additivity of the structure functions could be detected, other than those caused by Fermi motion. This additivity is an assumption made when comparing the data in this experiment to the predictions based on Monte Carlo calculations.

The realization of the scaling geometry is shown in

Fig. 1 for the two energies used in the experiment. The data reported in this letter was taken at only one target position for each energy, but additional data with other target positions exists and will be reported elsewhere. The momentum analyzing magnets are solid iron toroids 68 inches in diameter with an inner diameter of 12 inches and a thickness of 31 inches. The symmetry of the magnets produces a B field pointing along the azimuthal direction and acting to focus positive muons radially inward. A detailed study¹¹ was made of the variation of the magnetic field, which has an absolute uncertainty of $\pm 1\%$ and an uncertainty of $\pm 0.5\%$ in the radial field dependence.

A scattered muon trigger is defined by three counter banks having a hole in the center to prevent beam triggers. A fourth bank of counters is placed upstream of the target to veto accidental beam-halo coincidences. The beam size at the target is sharply defined by another veto counter. Beam muons or muons scattered through very small angles are vetoed by a coincidence of two veto counters labeled BV and BV' in Fig. 1. To prevent an accidental vetoing of real events the holes in each magnet are plugged with concrete.

Each spark chamber module (SC₇-SC₁₅ in Fig. 1) consists of four planes with magnetostrictive wands. Vertical and

horizontal coordinates are recorded as well as coordinates in the $\pm 45^\circ$ direction. To improve spatial uniformity the wands alternate in direction in alternate spark chamber modules.

The read-out system has a capacity of eight sparks or fiducials per wand plus an overflow indication.

A multiwire proportional counter system is used both to record the incident beam track and to locate the scattered track immediately downstream of the target. The beam track is located to ± 1.5 mm with the incident angle measured to ± 0.1 mrad. During energy calibration runs another proportional chamber is used upstream of the last bend in the muon beam line. This chamber is used to reset the beam energy to its nominal value and also allows a measurement of the muon beam momentum spectrum.

For some events, typically having a very high energy loss ν , the scattered muon track may be obscured by a hadronic or electromagnetic shower. To provide information on these events the target is segmented into 4-inch blocks with scintillation counters between each block. The pulse height in these counters is recorded and will ultimately be used to provide additional information on the location of the event vertex. This information is complementary to that provided by the proportional counters and spark chambers. In the results reported below

only information from the spark chambers located downstream of the first magnet in the spectrometer is used. The other information can be used to improve the spectrometer resolution. This will be done in a subsequent analysis.

Data was taken in August and October 1973 (150 GeV) and April 1974 (56 GeV). The results reported here are based on about 30% of the total data sample and only one position of the target. The use of different target positions (see Fig. 5) varies the acceptance below q^2 of 5 by a significant factor, allowing the collection of more data at large ω values. In the single target position used for the data reported here the q^2 range for an acceptance greater than 10% is less than 50 $(\text{GeV}/c)^2$. The mean ω value is about 9 and the mean q^2 about 14 $(\text{GeV}/c)^2$. The effective number of muons for the present data is approximately 0.80×10^9 at 150 GeV and 1.7×10^9 at 56 GeV. 98% of the 150 GeV beam and 91% of the 56 GeV beam is contained within a 9 cm radius and 2 milliradian divergence angle. In some of the data, notably the 150/56 ratio comparison, a 4.5 cm 1 milliradian beam cut was used. This provides a further reduction in the effective total flux to 0.43 and 1.0×10^9 at 150 and 56 GeV respectively. The beam spill was such that on the average about 5% of the events contained two beam tracks. Corrections were made to the flux

for veto dead time and loss in reconstructing proportional chamber beam tracks (a few percent in each case). The data rate (reconstructed events) was observed to remain constant over instantaneous beam intensities varying over at least one decade. The halo/beam ratio was typically 70% with a variation of a factor of two during the data taking. We find no evidence of rate dependence or halo contamination (from accidentals) in either the event yield or the q^2 distribution. The trigger rate was of the order of 10^{-5} per incident muon.

It was useful to trigger on beam tracks selected at random to monitor the beam geometrical characteristics and to provide an input sample to Monte Carlo simulations of the experiment. Periodically the beam was steered into the spectrometer to provide calibration data some of which is shown in Figs. 3 and 4.

Two different analysis efforts using different reconstruction algorithms but identical momentum fits were used. The results of these analyses were averaged to obtain the results used in Fig. 8, plotted in Fig. 8. A third analysis, also ~~also~~ used different point selection for the track reconstruction and a different procedure for momentum fitting. Differences between these analyses allow us to estimate that systematic errors which are analysis dependent are at the level of the statistical

errors quoted. This can be improved with more study of the analysis procedures.

One major problem in the analysis centered around the use of information from the spark chambers and proportional chambers located immediately downstream of the target. Showers initiated by high multiplicity events caused an average loss of "front" information 25-30% of the time,¹³ with an efficiency which is greatly reduced at low E' (high ν). Another manifestation of this effect was an energy dependent tail on the chi squared distribution for the momentum fits. Figure 6 shows a typical E' spectrum at fixed q^2 without corrections for these losses. It is believed that the additional events can be recovered by using the information given by pulse height analysis of the target counters but algorithms for doing this are still being developed. To produce the results of this paper, a fit was made using only information from the spark chambers downstream of the first spectrometer magnet. This changes the resolution of the spectrometer to $\approx 18\%$ in $1/E'$ (this quantity has a gaussian distribution).

The momentum fit takes into account multiple scattering and measurement errors and allows for error correlations between track positions measured in different modules.

Figure 7 shows the chi squared distribution for two different energies (56 GeV geometry) using only the downstream information. Our estimated measurement error of 0.5 mm is seen to be somewhat too large. The mean chi squared/degree of freedom is 1.05 at 56 GeV and 1.01 at 150 GeV with 0.7% and 1.6% of the events beyond a chi squared/degree of freedom of 5.

To check the absolute reconstruction efficiency, the number of events expected in the same q^2, ω range as that covered by SLAC was computed and compared with the number actually obtained, normalized to the effective muon flux. This test is actually quite stringent since it depends strongly on the number of events which overflow into this region due to the wide resolution curve of the spectrometer. The ratio of predicted events/observed events was 1.00 ± 0.05 at 150 GeV and 0.89 ± 0.07 at 56 GeV. The actual absolute reconstruction efficiencies would be expected to be at least this good.

As a measure of any observed violation of scale invariance, we can parameterize a hypothetical violation by

assuming $F_2(q^2, \omega) = \frac{N}{(1 + q^2/\Lambda^2)^2} F_2(\text{SLAC})$ where the function

$F_2(\text{SLAC})$ is derived from fits to the electron scattering data¹⁵ and scales (is a function only of ω at these energies).

Λ has the dimensions of a mass and provides a scale. Varying N allows us to vary the absolute normalization of the muon experiment relative to the SLAC electron scattering data. No

inference should be drawn concerning the actual validity of the above functional form for F_2 which is merely a convenient way of expressing the degree of scale breaking in the experiment. In particular, it should be noted that ω (or x) varies across the q^2 distribution plotted in Fig. 8 due to our experimental acceptance, thus making it difficult to distinguish possible types of scale breaking from each other given this information alone.

The main results of this experiment to date are plotted in Fig. 8 and the results of fits of the type discussed above are given in Table II. We see that the data to Monte Carlo comparison shows a statistically significant deviation from the extrapolated values expected using the hypothesis of scale invariance and the SLAC F_2 values.¹⁵ The tendency of the normalization to be greater than 1.0 probably indicates that the functional form of the deviation is not a correct description of the physical effects being observed, particularly since good agreement is obtained with the absolute normalization in the region overlapping the SLAC kinematic range. Very poor fits are obtained by either assuming $1/\Lambda^2 = 0$ or $N = 1.0$.

We note that if a cut is made to restrict the data to $\omega < 9$, a less rapid decrease with q^2 is observed.

The systematic errors in this type of comparison are estimated to be ~ 0.0040 $(\text{GeV}/c)^{-2}$ in $1/\Lambda^2$ and $\pm 10\%$ in the normalization. By taking the ratio of 150 GeV data to 56 GeV data we can eliminate the need to depend on the Monte Carlo calculation at the price of losing statistical accuracy. The radiative corrections, absolute reconstruction efficiency, exact shape of F_2 in iron all cancel out along with other purely experimental effects. Using this method we obtain a $1/\Lambda^2$ about 2 standard deviations from 0. This statistical limit could easily be improved by accumulation of more data since at the present level of intensity and reliability of the muon beam, the data presented here could be duplicated in a day.

In the future more care has to be paid to ensure the scale invariance of the analysis. This can partly be checked with Monte Carlo. (The intrinsic slope of the experiment in the ratio method is much smaller than the physical effects reported here.) The front information will eventually be used to get better momentum resolution. Some inconsistencies remain in the various 56 GeV analyses and affect the ratio comparison. For this reason all "ratio" numbers are to be regarded as preliminary.

We would like to express our deep appreciation to the staff of the Fermi National Accelerator Laboratory, in particular R. Orr, T. Yamanouchi, P. Limon and R. Huson who contributed much at an early time in the history of the accelerator. L. Litt has been helpful in the later stages of running and data analysis. One of us (L.H.) would like to express his appreciation to K. Wilson and D. Yennie for many useful discussions. We also thank the National Science Foundation for their generous support and encouragement throughout this experiment.

References

1. J. D. Bjorken, Phys. Rev. 179, 1547 (1969).
2. $q^2 = 4E_0'E \sin^2 \frac{\theta}{2}$
 $v = E_0 - E'$
 $\omega = 2mv/q^2$
3. E. D. Bloom et al., Phys. Rev. Lett. 23, 930 (1969);
 G. Miller, Phys. Rev. D5, 528 (1972).
4. R. P. Feynman, Phys. Rev. Lett. 23, 1415 (1969);
 unpublished. For a comprehensive survey of parton model
 predictions, see J. Kogut and L. Susskind, Physics
 Reports 8C, 2 (June 1973).
5. J. Kogut and L. Susskind, "Parton Models and Asymptotic
 Freedom" (1973 preprint); D. Gross and S. B. Treiman,
 Phys. Rev. Lett. 32, 1145 (1974).
6. These were largely the early availability of a muon beam
 simultaneously with the neutrino beam and the ease of
 detecting high energy muons.
7. Fermi National Accelerator Laboratory Experiment 26.
 Preliminary results were reported by K. W. Chen, Bull. Am.
 Phys. Soc. 19, (1), 100 (1974). Previous work on the deep
 inelastic scattering of muons done at Brookhaven and SLAC
 established that, relative to electron scattering:

In hydrogen $N = 0.997 \pm 0.043$

$$\frac{1}{\Lambda_\mu^2} - \frac{1}{\Lambda_e^2} = 0.0060 \pm 0.0160$$

In deuterium $N = 0.925 \pm 0.038$

$$\frac{1}{\Lambda_\mu^2} - \frac{1}{\Lambda_e^2} = -0.0190 \pm 0.0160$$

The hydrogen results are given by A. Entenberg et al., Phys. Rev. Lett. 32, 486 (1974). The deuterium results are given by J. Kim et al., to be published in Phys. Rev. Lett. The interpretation of the SLAC electron scattering data depends on the choice of scaling variable. With the choice of ω , $1/\Lambda_e^2 = 0.0150 \pm 0.0020$ (see Riordan's thesis). If $\omega' = \omega + (M^2/q^2)$ is chosen $1/\Lambda_e^2$ is "consistent with zero".

8. A detailed explanation of how the scaling apparatus works can be found in an internal memorandum entitled "Status Report - Experiment 26", submitted to the Program Advisory Committee June 11, 1974. All measured coordinates in the experiment have the same average value and distributions if F_2 and R scale. Corrections to this statement have been studied and are almost negligible.
9. H. W. Kendall, invited talk, Proceedings of 1971 International Symposium on Electron and Photon Interactions at

High Energies, Cornell University (Laboratory of Nuclear Studies, Cornell Univ., Ithaca, N.Y., 1972).

10. L. Lederman, private communication. Analysis of this work is still in progress.
11. See the E26 Status Report referred to in Ref. 8.
12. This system follows a design originated by D. Hartill of Cornell Univ.
13. See E26 Status Report, Ref. 8, for details of how this is measured.
14. The average value of ω being sampled by the apparatus varies with q^2 , from > 16 for $q^2 < 10$ to ~ 2 for $q^2 > 40$.
15. A. Bodek, M.I.T. Ph.D. thesis (1972); M. Riordan, M.I.T. Ph.D. thesis (1973).

Table I. Assumptions in Comparing Data with Monte Carlo

1. MUONS=ELECTRONS
2. ν_{H_2} FROM BODEK'S FIT TO THE SLAC DEUTERIUM AND HYDROGEN DATA.
IRON = 26 DEUTERONS + 4 NEUTRONS
3. R=.168
4. NUCLEON FERMI MOTION-THOMAS FERMI GAS MODEL
5. RADIATIVE CORRECTIONS USING AN EQUIVALENT RADIATOR APPROXIMATION.
ADDITIONAL CORRECTIONS USING VERTEX CORRECTION AND VACUUM
POLARIZATION WILL AFFECT THE ABSOLUTE NORMALIZATION BY A FEW
PERCENT AND ARE NOT YET MADE.
6. MULTIPLE SCATTERING IN BOTH TARGET AND SPECTROMETER. GAUSSIAN
APPROXIMATION
7. ENERGY DEPENDENT dE/dx CORRECTION
8. 1MM SPATIAL RESOLUTION
9. MAGNETIC FIELD IN SPECTROMETER MEASURED WITH FLUX LOOPS AND
ALSO DETERMINED FROM THE B-H CURVE OF THE IRON. FITTED TO A
4 PARAMETER FIT. THE DEGAUSSING WAS CHECKED DIRECTLY AND ALSO
WITH HALO MUONS.
10. THE MONTE CARLO ASSUMED THE BEAM SHAPE OBTAINED BY SAMPLING THE
BEAM THROUGH THE PROPORTIONAL CHAMBERS CONCURRENTLY WITH THE
DATA ACCUMULATION.

Table II. Results of Fits to Data in Fig. 8

	Data Sample	Ref. Fig. 8	N	$\frac{1}{\Lambda^2}$ in $(\text{GeV}/c)^{-2}$	χ^2/n_D	Confidence Level	Remarks
Absolute =	150 GeV	g	$1.30 \pm .06$	$.0083 \pm .0015$	5.5/7	61%	
<u>Data</u> Monte Carlo	150 GeV, $\omega < 9$	h	$1.10^{+.10}_{-.06}$	$.0042^{-.0015}_{+.0028}$	3.5/7	83%	"Loose" Beam
	56 GeV	i	$1.10 \pm .03$	$.0110(\sim \pm .0020)$	7/7	44%	
	150 GeV/56 GeV	f	$1.10 \pm .10$	$.0120 \pm .0060$	1.1/5	94%	"Tight" Beam, No corrections Note χ^2 is low
Ratio =	150 GeV/56 GeV	g,i	$1.20^{+.10}_{-.07}$	$.0106^{+.0060}_{-.0040}$	7.8/7	37%	"Loose" Beam, Correction from ratio of Monte Carlos at 56 and 150 GeV
<u>Data</u> <u>Data</u>			0.997 $\pm .028$	0	15.3/8	12%	Fit to a constant

Figure Captions

Fig. 1 Apparatus for the scaling test. SC = spark chamber, PC = proportional chamber, SA,SB,SC = counter hodoscope, and HV,BV = veto counters.

Fig. 2 Expanded view of target cart geometry.

Fig. 3 Spectrometer calibration.

Fig. 4 Linearity of spectrometer calibration and percent resolution in $1/E'$.

Fig. 5 Raw data showing the effect of changing target position at fixed muon energy. Only the 180" data is reported in this paper.

Fig. 6 E' spectrum at fixed q^2 using the front chamber information. These data are without correction for losses due to hadron showers. Also shown are the predictions for perfect resolution and 14% resolution using the SLAC F_2 extrapolated to these energies.

Fig. 7 Chi squared distribution of fits using only the information from the shielded spark chambers in the rear of the spectrometer. In this case the resolution in $1/E'$ is about 18%, but almost all effects due to hadron showers are removed.

Fig. 8 Results of the comparison of 56 GeV data with 150 GeV data vs. q^2 and of each energy separately compared to Monte Carlo simulation of the experiment.

(a), (b), (c), (d) are the actual observed q^2 distributions for 150 GeV "tight beam", 56 GeV "tight beam", 150 GeV "loose beam" and 150 GeV Monte Carlo "loose beam". "Tight beam" refers to restricting the incident muons to a radius of 4.5 cm and 1.0 milliradian divergence, "loose beam" to a beam cut at 9.0 cm and 2.0 milliradian divergence. (e) is the detection efficiency plotted vs. q^2 . (f) is the ratio comparison 150 GeV data/56 GeV data with tight beam cuts, (g) the ratio of 150 GeV data to Monte Carlo with loose beam cuts, (h) the same but for $\omega < 9$, and (i) the ratio of 56 GeV data to Monte Carlo with loose beam. The errors shown in all cases are statistical errors only.

Fig. 9 Effects of various types of systematic errors and the radiative correction.

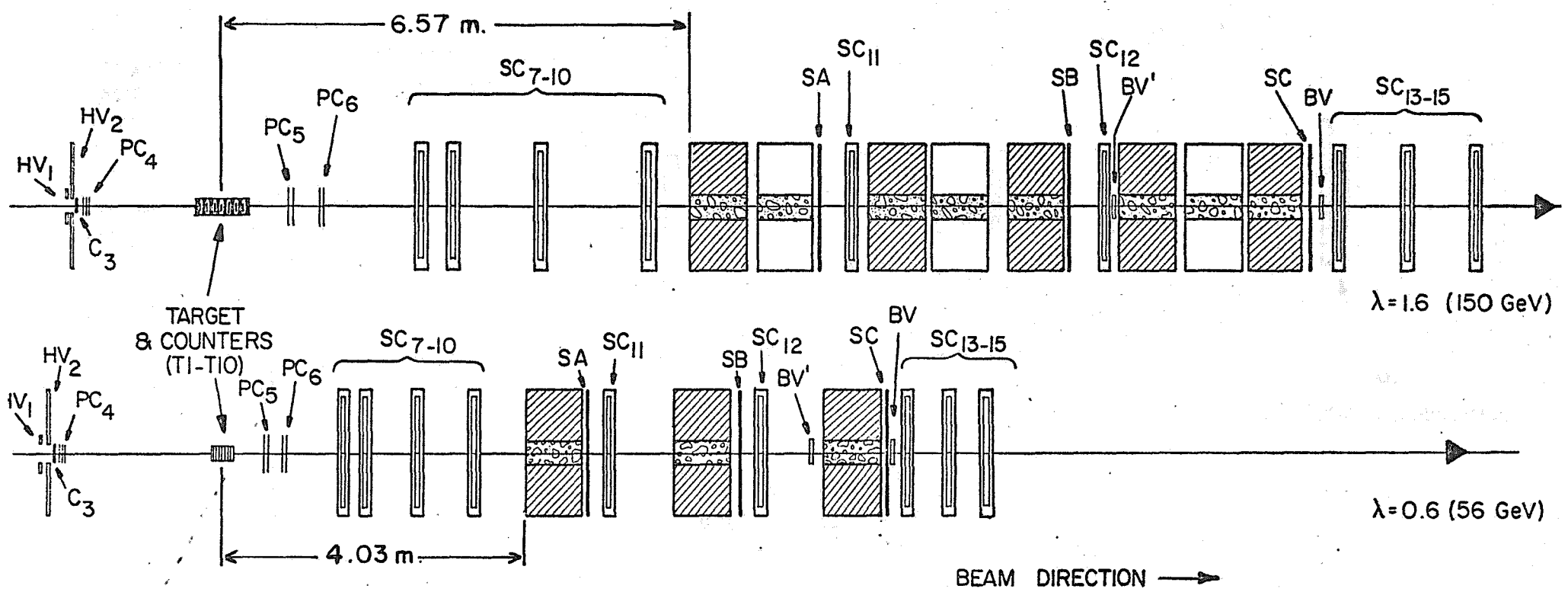


FIG. 1

TARGET CART GEOMETRY
(at 150 GeV)

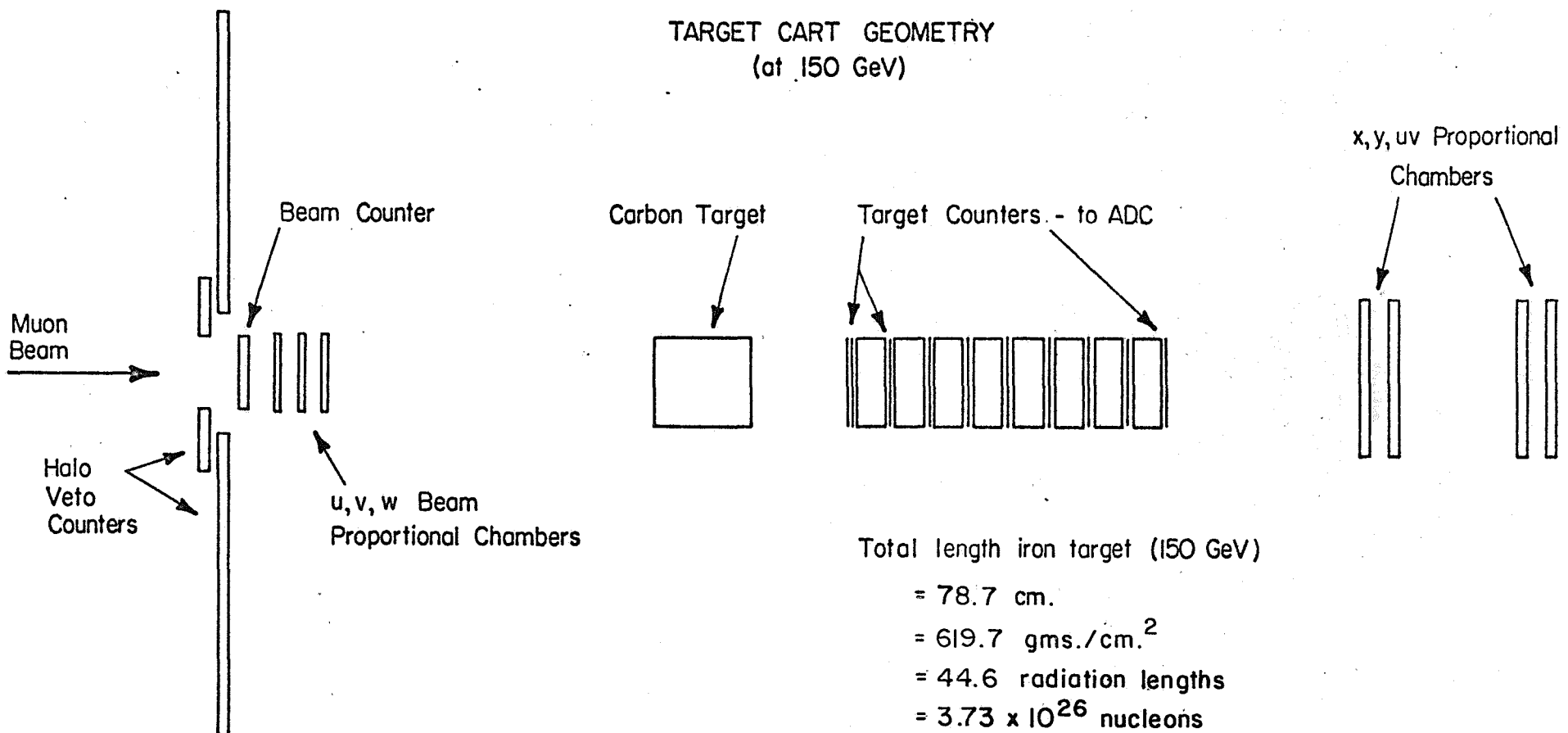
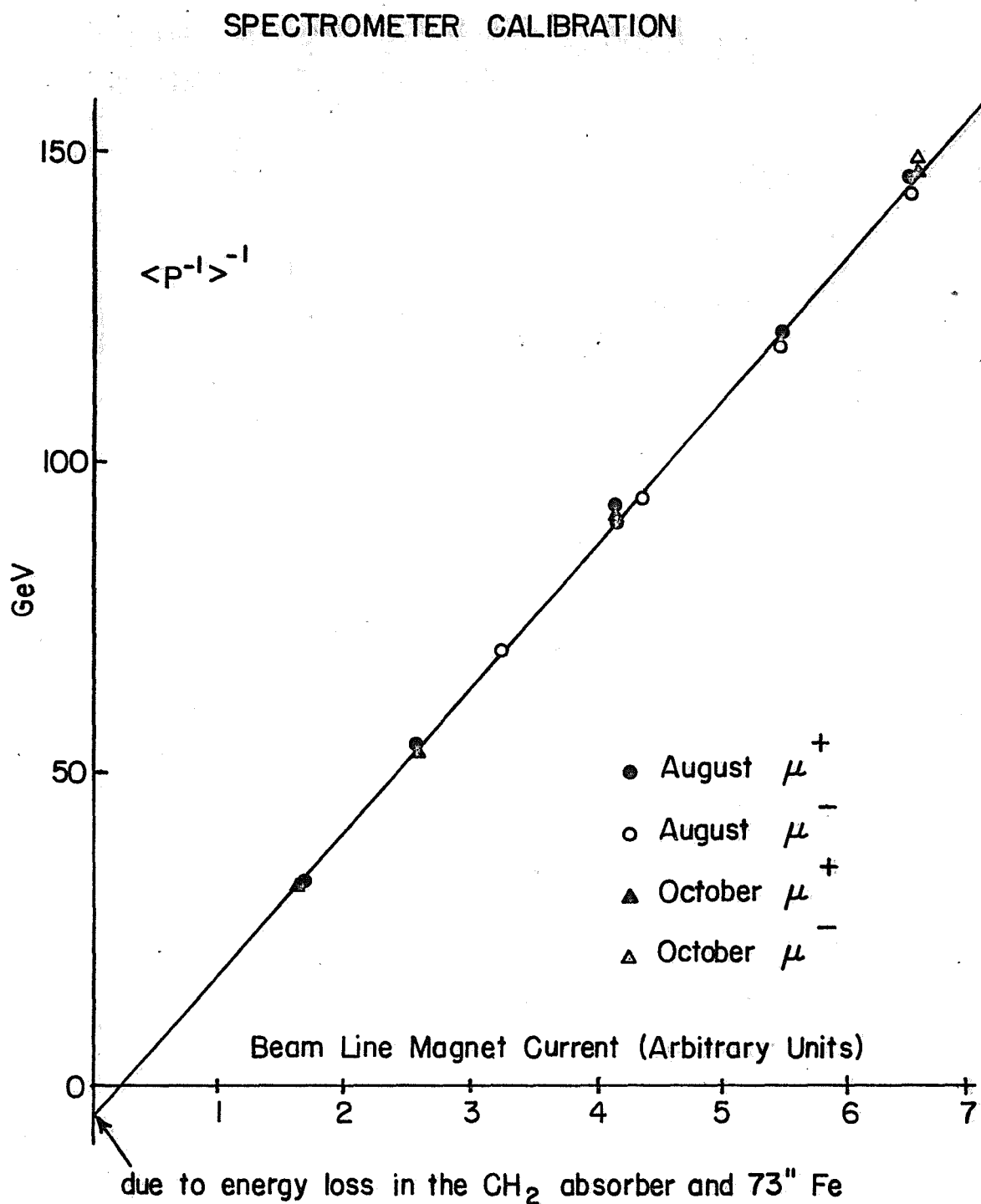


FIG. 2

Feb. 1974



0290574

FIG. 3

Feb. 1974

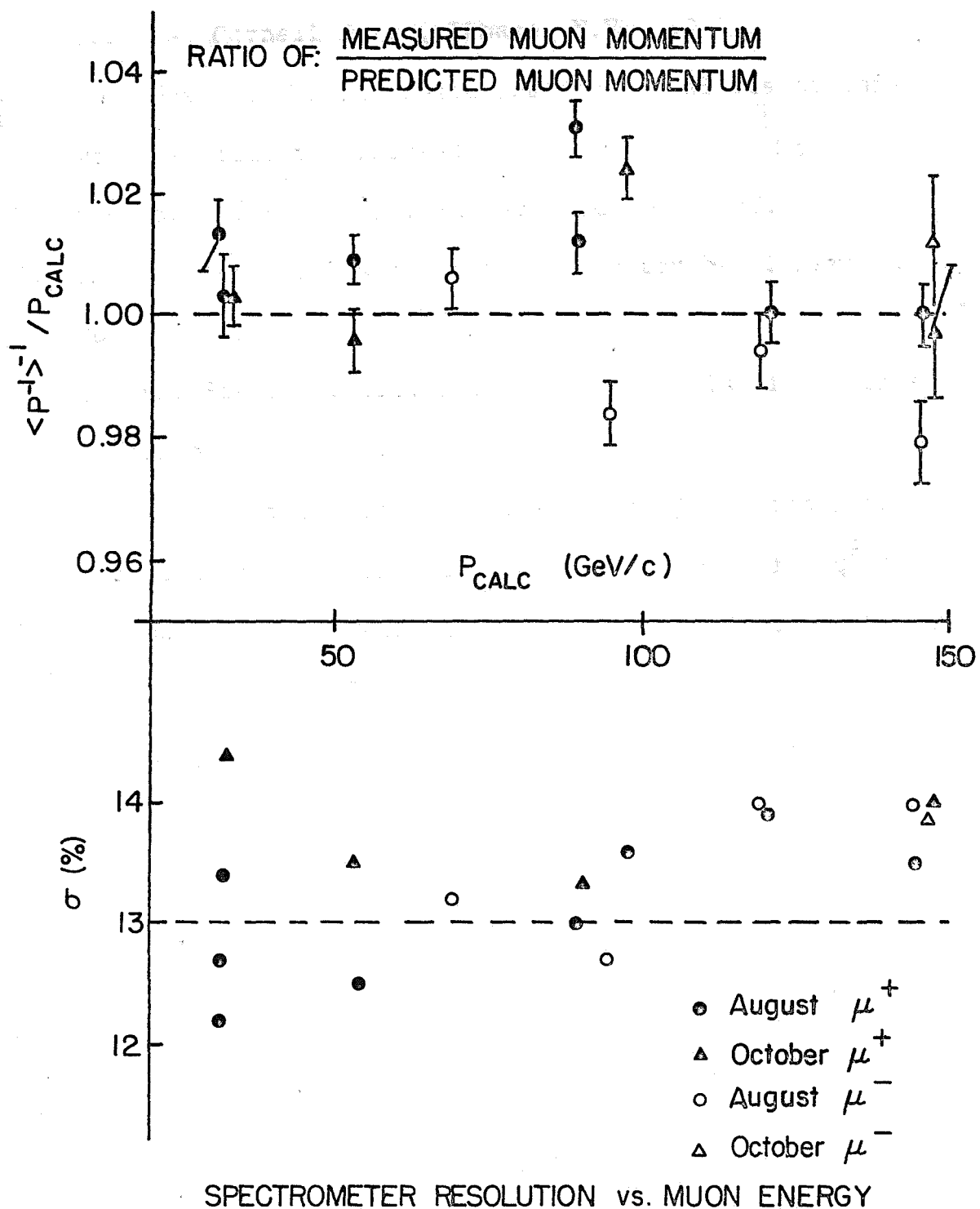


FIG. 4

0290574

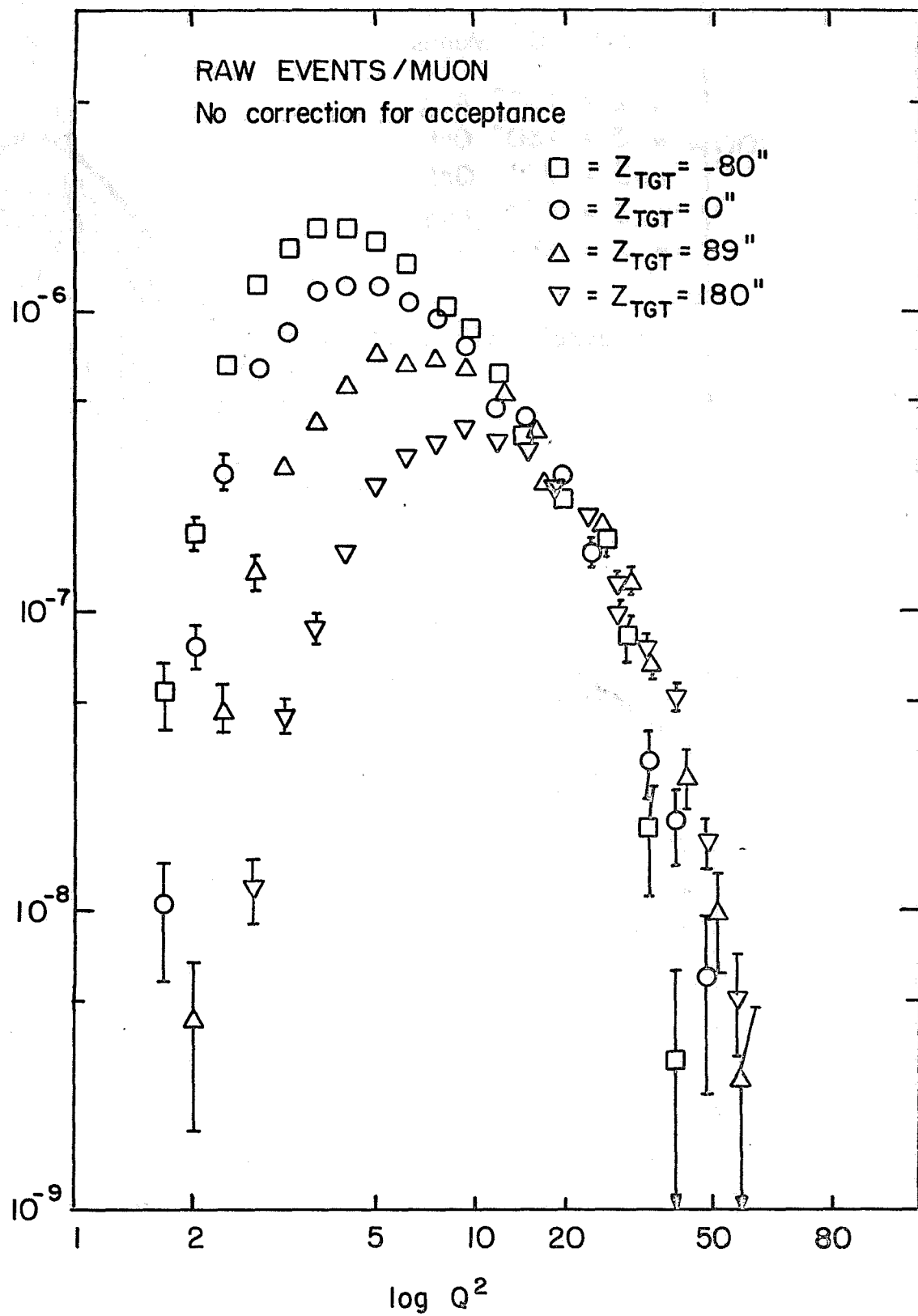


FIG. 5

0290574

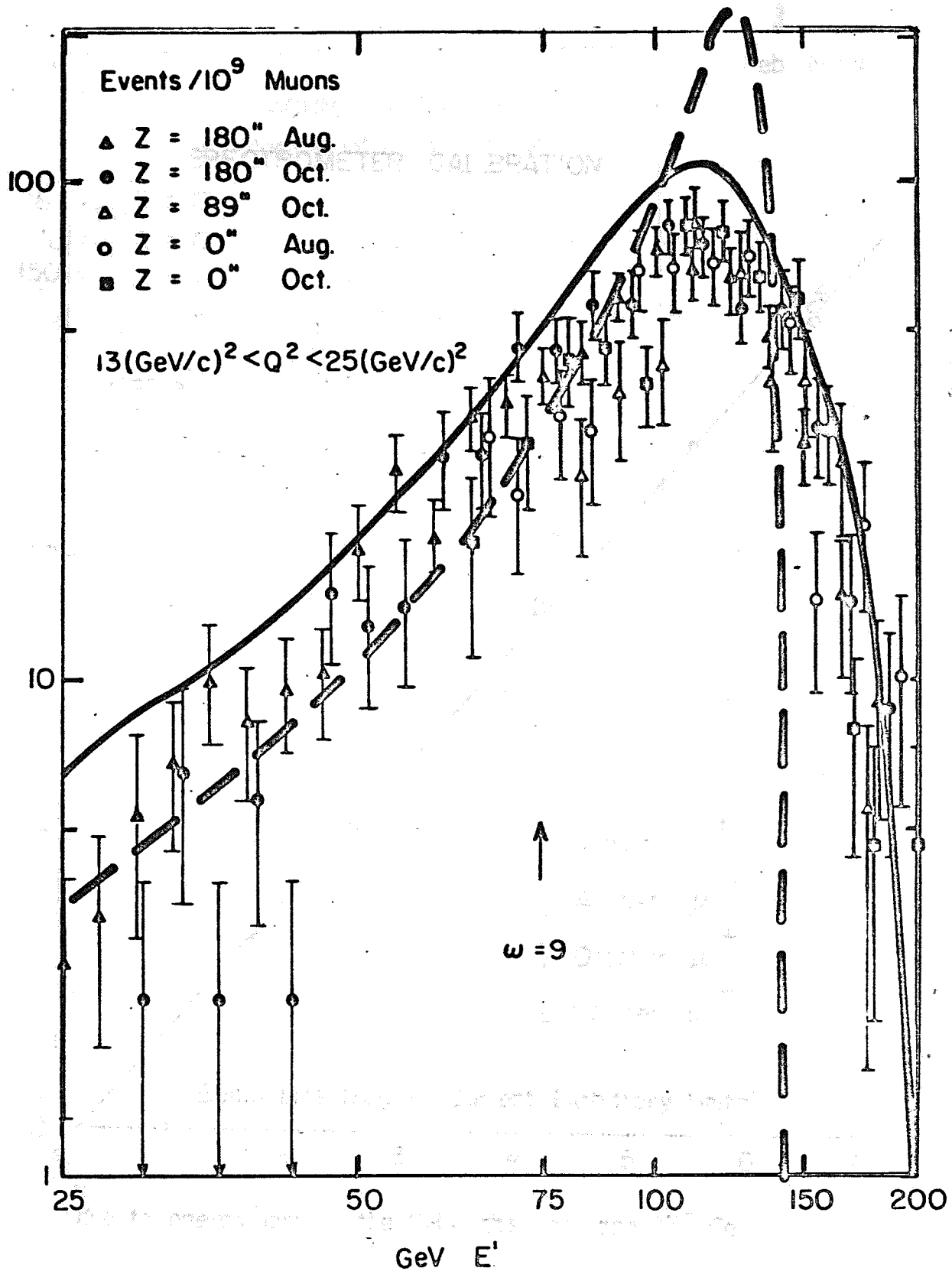
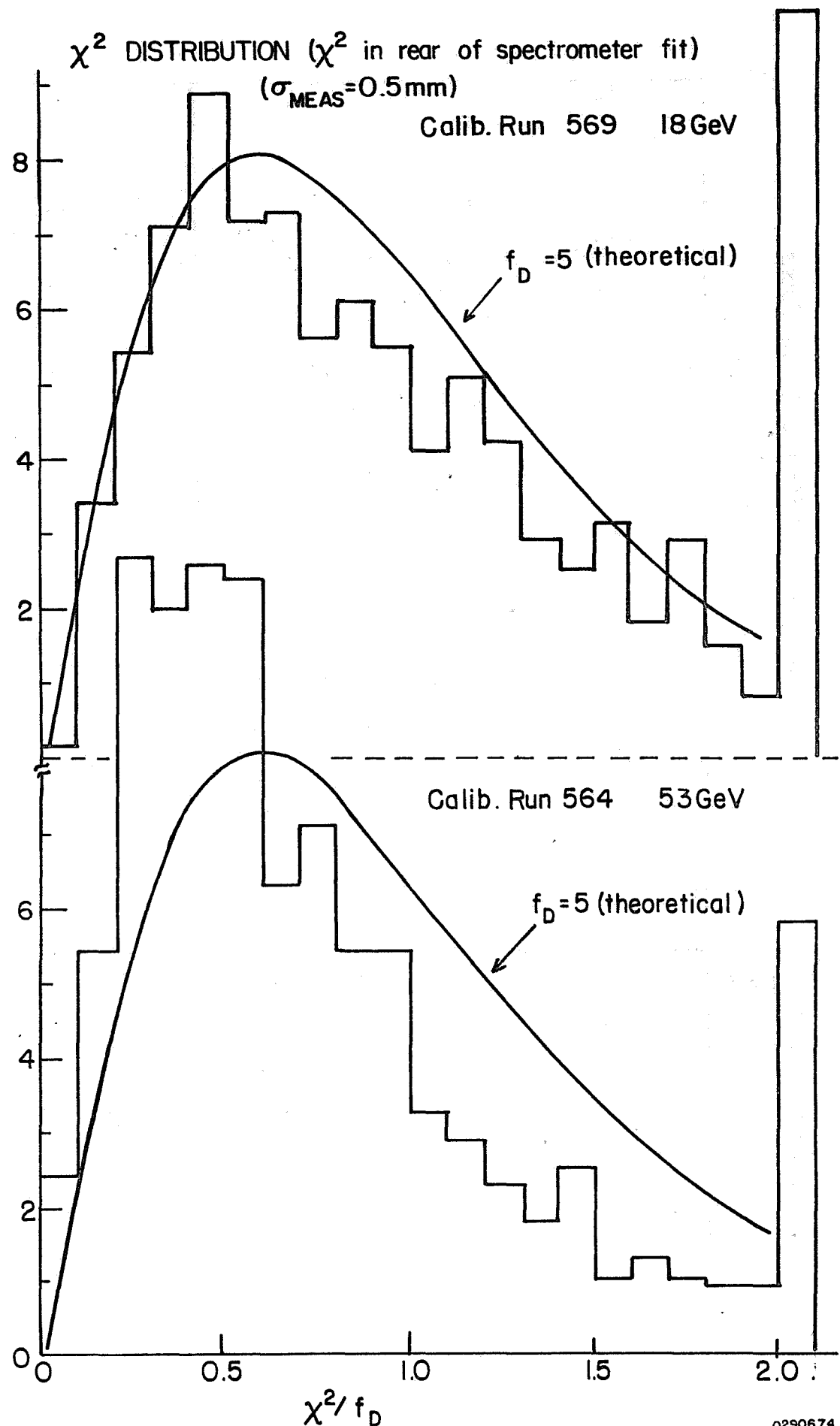


FIG. 6

$13 < Q^2 < 25$

0290274



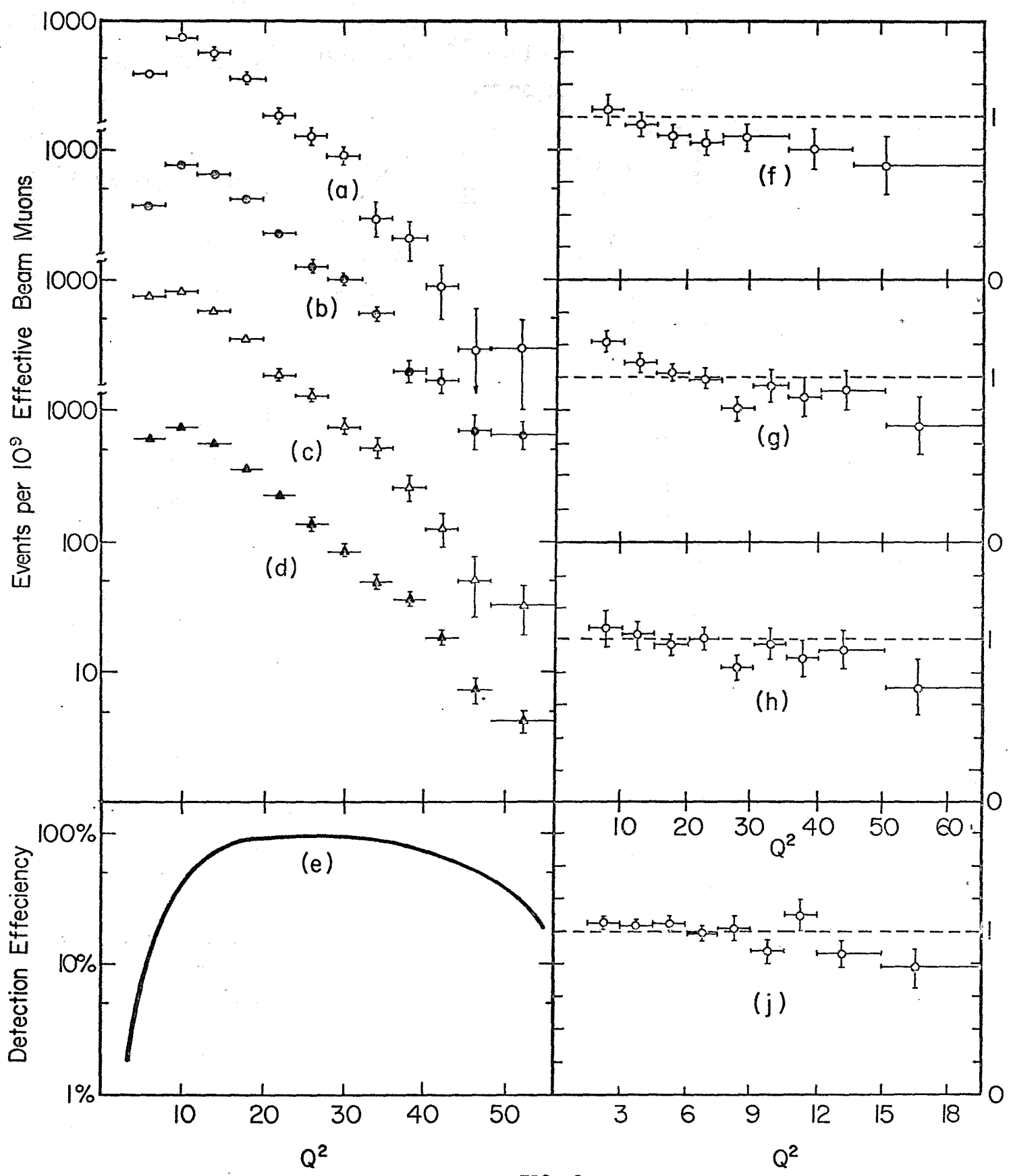


FIG. 8

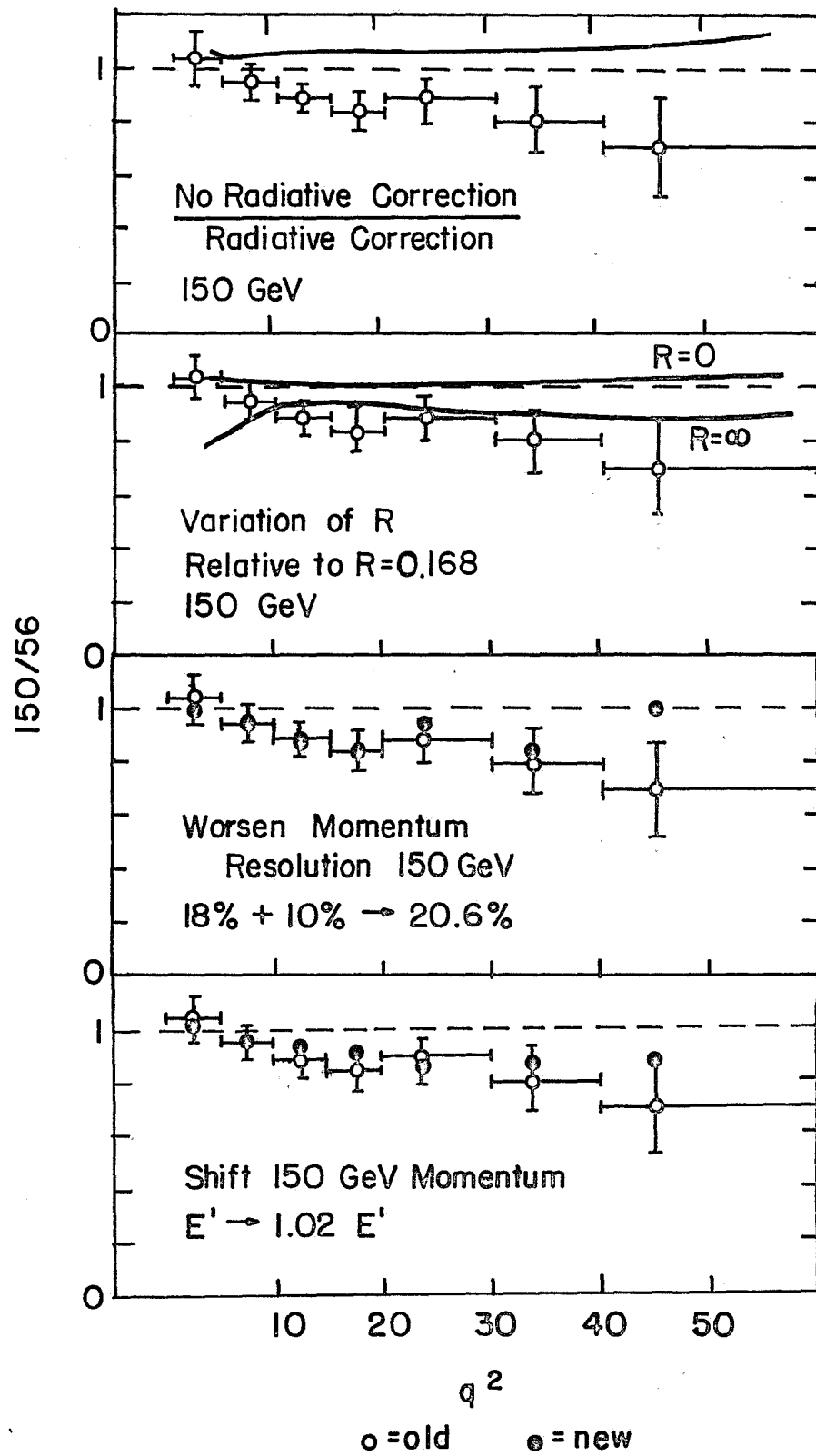


FIG. 9

0290674